# Gas-Phase Reactions of $Fe(CH_2O)^+$ and $Fe(CH_2S)^+$ with Small Alkanes: An Experimental and Theoretical Study

**Quan Chen, Huiping Chen, Sabre Kais,* and Ben S. Freiser***

*Contribution from the H. C. Brown Laboratory of Chemistry, Purdue University, West Lafayette, Indiana 47907*

*Received December 9, 1996*[⊗]

**Abstract:** The gas-phase reactions of $Fe(CH_2O)^+$ and $Fe(CH_2S)^+$ with a series of aliphatic alkanes were studied by Fourier transform ion cyclotron resonance (FTICR) mass spectrometry. Like bare $Fe^+$, C−C insertion, particularly terminal C−C insertion, is predominant for the reactions of $Fe(CH_2O)^+$, while C−H insertion is preferred for $Fe(CH_2S)^+$. About 90% of the $Fe(CH_2O)^+$ reaction products are formed by C−C insertion with small alkane loss. For $Fe(CH_2S)^+$, after initial C−H insertion, the proposed mechanism includes hydrogen transfer to sulfur, followed by migratory insertion of methylene into the metal−alkyl bond and formation of an activated $H_2S-Fe^+$−olefin complex, which dissociates by $H_2S$ elimination. The structures of the reaction products were probed by collision-induced dissociation, ion−molecule reactions, and use of labeled compounds, yielding information about the reaction mechanism. Collision-induced dissociation and ligand displacement reactions yield the brackets $D^0(Fe^+-C_3H_6) = 37 \pm 2$ kcal/mol $< D^0(Fe^+-CH_2S) < D^0(Fe^+-C_6H_6) = 49.6 \pm 2.3$ kcal/mol and $D^0(Fe^+-CH_2O) < D^0(Fe^+-C_2H_4) = 34 \pm 2$ kcal/mol. The optimized geometry of $Fe(CH_2O)^+$, obtained by density functional calculations, has $C_{2v}$ symmetry with a nearly undisturbed formaldehyde unit. The $Fe^+-CH_2O$ bonding is found to be predominantly electrostatic with a calculated bond energy of 32.2 kcal/mol. However, the optimized $Fe(CH_2S)^+$ structure has $C_s$ symmetry with dative bonding between $Fe^+$ and $CH_2S$. $D^0(Fe^+-CH_2S)$ is calculated at 41.5 kcal/mol. The differences in geometry and chemical bonding between $Fe(CH_2O)^+$ and $Fe(CH_2S)^+$ are correlated with the different reaction pathways observed.

## Introduction

The gas-phase reactions of atomic transition metal ions have been the focus of intense investigation for the past 20 years, yielding a great deal of information on "intrinsic" properties, such as kinetics, thermochemistry, and reaction mechanisms in the absence of solvation and counterion effects.[1] The reactions with simple hydrocarbons have been particularly important, because they are closely related to solution organometallic chemistry and catalysis. Since there are only two types of bonds in alkanes available for metal ion insertion, C−C bonds and C−H bonds, the reactions with alkanes provide an ideal system for the study of $\sigma$-bond activation.[2]

Previous studies have shown that the reactivity of a gas-phase metal ion is dramatically changed by the addition of a ligand. Furthermore, the overall reactivity of a metal ion can be either increased or decreased by the presence of a ligand. While $M^+$ (M = Fe, Co, Ni) reacts with alkanes predominantly by oxidative insertion into C−C bonds,[3−7] C−H insertion occurs exclusively in the reactions of $MD^+$ (M = Fe, Co, Ni),[8−12] $MO^+$ (M = Fe, Co),[13−18] $MS^+$ (M = Fe, Co, Ni),[19] and $MCH_2^+$ (M = Fe, Co) with small alkanes.[20] For example, $FeO^+$ reacts with small alkanes primarily by initial C−H insertion to generate an activated $H_2O-Fe^+$−olefin complex, which subsequently decomposes to lose $H_2O$.[13] Similarly, $FeS^+$ reacts with hydrocarbons by C−H bond insertion, leading to $H_2S$ loss and subsequent dehydrogenation.[19] Armentrout and co-workers have recently reported that, while $Fe(CO)^+$ activates C−H and C−C bonds almost equally, $Fe(H_2O)^+$ preferentially activates C−H bonds.[21] They also concluded that $\pi$ back-donation from $H_2O$ enhances $\sigma$-bond activation ability, while the $\pi$-accepting CO ligand suppresses the activation of $\sigma$-bonds.

In this paper the gas-phase reactions of $Fe(CH_2O)^+$ and $Fe(CH_2S)^+$ with a series of aliphatic alkanes are studied by Fourier transform ion cyclotron resonance (FTICR) mass spectrometry. The goal of this study was 3-fold: to determine the ligand effects of $CH_2O$ and $CH_2S$ on the reactivity of $Fe^+$; to determine metal−ligand bond energies; and to explore the chemical

[⊗] Abstract published in *Advance ACS Abstracts,* December 15, 1997.

(1) (a) Russell, D. H., Ed. *Gas-Phase Inorganic Chemistry*; Plenum Press: New York, 1989. (b) Eller, K.; Schwarz, H. *Chem. Rev.* **1991**, *91*, 1121. (c) Freiser, B. S. *Acc. Chem. Res.* **1994**, *27*, 353. (d) Freiser, B. S., Ed. *Organometallic Ion Chemistry*; Kluwer Academic Publishers: Dordrecht, 1996. (e) Freiser, B. S. *J. Mass Spectrom.* **1996**, *31*, 703.

(2) van Koppen, P. A. M.; Bowers, M. T.; Fisher, E. R.; Armentrout, P. B. *J. Am. Chem. Soc.* **1994**, *116*, 3780.

(3) Allison, J.; Freas, R. B.; Ridge, D. P. *J. Am. Chem. Soc.* **1979**, *101*, 1332.

(4) Jacobson, D. B.; Freiser, B. S. *J. Am. Chem. Soc.* **1983**, *105*, 5197.

(5) Halle, L. F.; Houriet, R.; Kappes, M. M.; Staley, R. H.; Beauchamp, J. L. *J. Am. Chem. Soc.* **1982**, *104*, 6293.

(6) Georgiadis, R.; Fisher, E. R.; Armentrout, P. B. *J. Am. Chem. Soc.* **1989**, *111*, 4251.

(7) Freas, R. B.; Ridge, D. P. *J. Am. Chem. Soc.* **1980**, *102*, 7129.

(8) Houriet, R.; Halle, L. F.; Beauchamp, J. L. *Organometallics* **1983**, *2*, 1818.

(9) Carlin, T. J.; Sallans, L.; Cassady, C. J.; Jacobson, D. B.; Freiser, B. S. *J. Am. Chem. Soc.* **1983**, *105*, 6320.

(10) Elkind, J. L.; Armentrout, P. B. *J. Phys. Chem.* **1986**, *90*, 5736.

(11) Jacobson, D. B.; Freiser, B. S. *J. Am. Chem. Soc.* **1985**, *107*, 4373.

(12) Halle, L. F.; Klein, F. S.; Beauchamp, J. L. *J. Am. Chem. Soc.* **1984**, *106*, 2543.

(13) Jackson, T. C.; Jacobson, D. B.; Freiser, B. S. *J. Am. Chem. Soc.* **1984**, *106*, 1252.

(14) Schröder, D.; Schwarz, H. *Angew. Chem., Int. Ed. Engl.* **1990**, *29*, 1443.

(15) (a) Shaik, S.; Danovich, D.; Fiedler, A.; Schröder, D.; Schwarz, H. *Helv. Chim. Acta* **1995**, *78*, 1393. (b) Schröder, D.; Wesendrup, R.; Schalley, C. A.; Zummack, W.; Schwarz, H. *Helv. Chim. Acta* **1996**, *79*, 123.

(16) Clemmer, D. E.; Aristov, N.; Armentrout, P. B. *J. Phys. Chem.* **1993**, *97*, 544.

(17) Clemmer, D. E.; Chen, Y.-M.; Khan, F. A.; Armentrout, P. B. *J. Phys. Chem.* **1994**, *98*, 6522.

(18) Chen, Y.-M.; Clemmer, D. E.; Armentrout, P. B. *J. Am. Chem. Soc.* **1994**, *116*, 7815.

(19) Jackson, T. C.; Carlin T. J.; Freiser, B. S. *Int. J. Mass Spectrom. Ion Proc.* **1986**, *72*, 169.

(20) Jacobson, D. B.; Freiser, B. S. *J. Am. Chem. Soc.* **1984**, *106*, 3891.

(21) Tjelta, B. L.; Armentrout, P. B. *J. Am. Chem. Soc.* **1996**, *118*, 9652.

S0002-7863(96)04234-5 CCC: $14.00 

bonding differences between $Fe(CH_2O)^+$ and $Fe(CH_2S)^+$. To do this, product ion structures were probed by collision-induced dissociation, specific ion−molecule reactions, and use of labeled compounds, and experimental bond energies were obtained by using ion−molecule bracketing and competitive collision-induced dissociation methods.

Formaldehyde was chosen since it is the simplest hydrocarbon containing oxygen, and an understanding of its ligand effects on $Fe^+$ may provide information on the mechanism of hydroformylation and many other catalytic processes, such as those involved in the synthesis of aldehydes and other oxygenated products.[22−24] Also, the electronic spectroscopies of both formaldehyde[25] and thioformaldehyde[26−28] have been widely studied, both experimentally and theoretically, due to their simplicity and few vibrational degrees of freedom. The extensive spectroscopic information provides supplemental information useful in explaining the chemical bonding between $Fe^+$ and both $CH_2O$ and $CH_2S$.

Finally, theoretical calculations are performed to determine the geometries and bonding configurations of both ligated species. There is growing evidence that modern density functional theory (DFT) is capable of meeting the challenges and providing a unified theoretical framework for the study of the electronic, geometric, and vibrational structures of transition metal systems.[29,30] Here we examine $Fe(CH_2O)^+$ and $Fe(CH_2S)^+$ by both HF and DFT with different basis sets. The results are used to explain the chemical bonding nature of both species and to provide an estimate of the metal−ligand bond energies. The calculated $Fe^+-CH_2O$ bond energy, together with the experimental value, is compared to those obtained previously by Schwarz[31] and Armentrout[32] and their co-workers.

## Experimental Section

All of the experiments were performed with a Nicolet (now Finnigan FT/MS, Madison, WI) prototype FTMS-1000 Fourier transform ion cyclotron resonance (FTICR) mass spectrometer, equipped with a 5.2 cm cubic trapping cell situated between the poles of a Walker Scientific 15-in. electromagnet, which was maintained at 1 T.[33] The cell has two 80% transmittance stainless steel mesh transmitter plates, and one of them holds various metal targets. Laser desorption ionization was used to generate $Fe^+$ from the pure iron foil by focusing the fundamental wavelength (1064 nm) of a Quanta-Ray Nd:YAG laser on the metal target.[34]

Chemicals, obtained commercially in high purity, were used as supplied except for multiple freeze−pump−thaw cycles to remove the noncondensable gases. Argon was present at a static background pressure of $\sim 1.0 \times 10^{-5}$ Torr, serving as a cooling gas to thermalize the ions prior to reactions, and at a total pressure of $\sim 2.0 \times 10^{-5}$ Torr as the collision gas in collision-induced dissociation (CID) experiments.[35] The cell pressure was monitored with a Bayard-Alpert ionization gauge.

**Table 1.** Product Distributions for the Reactions of $Fe(CH_2O)^+$ with Linear and Branched Alkanes

| | products | | |
|---|---|---|---|
| alkane | ion | ion percentage | neutral loss |
| methane | no reaction | | |
| ethane | no reaction | | |
| propane | $FeC_3H_6O^+$ | 96 | $CH_4$ |
| | $FeC_4H_8O^+$ | 4 | $H_2$ |
| [2,2-$D_2$]propane | $FeC_3H_4D_2O^+$ | 100 | $CH_4$ |
| *n*-butane | $FeC_4H_8O^+$ | 90 | $CH_4$ |
| | $FeC_5H_{10}O^+$ | 8 | $H_2$ |
| | $FeC_4H_8^+$ | 2 | $CH_2O$, $H_2$ |
| *n*-pentane | $FeC_5H_{10}O^+$ | 91 | $CH_4$ |
| | $FeC_6H_{12}O^+$ | 8 | $H_2$ |
| | $FeC_5H_{10}^+$ | 1 | $CH_2O$, $H_2$ |
| 2-methylpropane | $FeC_4H_8O^+$ | 91 | $CH_4$ |
| | $FeC_5H_{10}O^+$ | 9 | $H_2$ |
| 2,2-dimethylpropane | $FeC_5H_{10}O^+$ | 100 | $CH_4$ |
| 2-methylbutane | $FeC_5H_{10}O^+$ | 95 | $CH_4$ |
| | $FeC_6H_{12}O^+$ | 5 | $H_2$ |
| *n*-hexane | $FeC_5H_{10}O^+$ | 53 | $C_2H_6$ |
| | $FeC_6H_{12}O^+$ | 34 | $CH_4$ |
| | $FeC_7H_{14}O^+$ | 8 | $H_2$ |
| | $FeC_6H_{12}^+$ | 5 | $CH_2O$, $H_2$ |
| *n*-heptane | $FeC_6H_{12}O^+$ | 53 | $C_2H_6$ |
| | $FeC_6H_{10}O^+$ | 21 | $C_2H_6$, $H_2$ |
| | $FeC_5H_{12}O^+$ | 16 | $C_3H_6$ |
| | $FeC_7H_{14}O^+$ | 10 | $CH_4$ |
| *n*-octane | $FeC_7H_{14}O^+$ | 100 | $C_2H_6$ |
| *n*-nonane | $FeC_8H_{16}O^+$ | 93 | $C_2H_6$ |
| | $FeC_7H_{14}O^+$ | 3 | $C_3H_8$ |
| | $FeC_9H_{18}O^+$ | 4 | $CH_4$ |
| *n*-decane | $FeC_7H_{14}O^+$ | 96 | $C_4H_{10}$ |
| | $FeC_9H_{18}O^+$ | 4 | $C_2H_6$ |

$Fe(CH_2S)^+$ was formed by reacting $Fe^+$ with dimethyl sulfide, reaction 1,[19] which was introduced into the vacuum chamber through a General Valve Corporation Series 9 pulsed solenoid valve.[36] $Fe(CH_2O)^+$ was synthesized by reacting $Fe^+$ with pulsed-in dimethyl ether in a similar fashion, reaction 2. Observation of these two reactions

$$Fe^+ + CH_3SCH_3 \rightarrow Fe(CH_2S)^+ + CH_4 \quad (1)$$

$$Fe^+ + CH_3OCH_3 \rightarrow Fe(CH_2O)^+ + CH_4 \quad (2)$$

implies $D^0(Fe^+-CH_2O) > 0.2$ kcal/mol and $D^0(Fe^+-CH_2S) > 16.2$ kcal/mol, respectively.[37] Both $Fe(CH_2O)^+$ and $Fe(CH_2S)^+$ ions were collisionally cooled for 400 ms prior to isolation by swept double resonance techniques,[38] and then allowed to react with the alkane neutrals which were introduced into the cell by a second pulsed valve at a maximum of $\sim 1 \times 10^{-6}$ Torr. The primary product ion structures were investigated by collision-induced dissociation (CID) and ion−molecule reactions. The maximum translational energy acquired during CID by the ions is given in the laboratory frame and was calculated by using the following equation:[39,40]

$$E_{tr}(\max) = \frac{E_{RF}^2 q^2 t^2}{16 M_{ion}}$$

where $E_{RF}$ is the electric field amplitude, $t$ is the duration of the electric field applied, $q$ is the charge of the ion, and $M_{ion}$ is the mass of the ion to be excited.

(22) Lafyatis, D. S.; Creten, G.; Froment, G. F. *Appl. Catal. A* **1994**, *120*, 85.
(23) Hung, W. H.; Bernasek, S. L. *Surf. Sci.* **1996**, *346*, 165.
(24) Ivanov, K. *Appl. Catal. A* **1994**, *116*, L1.
(25) Moule, D. C.; Walsh, A. D. *Chem. Rev.* **1975**, *75*, 67.
(26) Johnson, D. R.; Powell, F. X. *Science* **1970**, *169*, 679.
(27) Clouthier, D. J.; Ramsay, D. A. *Annu. Rev. Phys.Chem.* **1983**, *34*, 31.
(28) Martin, J. M. L.; Francois, J. P.; Gijbels, R. *J. Mol. Specrosc.* **1994**, *168*, 363.
(29) Holthausen, M. C.; Fiedler, A.; Schwarz, H.; Koch, W. *J. Phys. Chem.* **1996**, *100*, 6236.
(30) Labanowski, J. K.; Andzelm, J. W. *Density Functional Methods in Chemistry*; Springer-Verlag: New York, 1991.
(31) Schröder, D.; Schwarz, H. *J. Organomet. Chem.* **1995**, *504*, 123.
(32) Tjelta, B. L.; Armentrout, P. B. *J. Phys. Chem. A* **1997**, *101*, 2064.
(33) Freiser, B. S. *Talanta* **1985**, *32*, 697.
(34) Cody, R. B.; Burnier, R. C.; Reents, W. D., Jr.; Carlin, T. J.; McCrery, D. A.; Lengel, R. K.; Freiser, B. S. *Int. J. Mass Spectrom. Ion Proc.* **1980**, *33*, 37.
(35) Burnier, R. C.; Cody, R. B.; Freiser, B. S. *J. Am. Chem. Soc.* **1982**, *104*, 7436.
(36) Carlin, T. J.; Freiser, B. S. *Anal. Chem.* **1983**, *55*, 571.
(37) Lias, S. G.; Bartmess, J. E.; Liebman, J. F.; Holmes, J. L.; Levin, R. D.; Mallard, W. G. Gas-Phase Ion and Neutral Thermochemistry. *J. Phys. Chem. Ref. Data*, **1988**, *17*, Suppl. No. 1.
(38) Comisarow, M. B.; Grassi, V.; Parisod, G. *Chem. Phys. Lett.* **1978**, *57*, 413.
(39) Grosshans, P. B.; Marshall, A. G. *Anal. Chem.* **1991**, *63*, 2057.
(40) Freiser, B. S. In *Techniques for the Study of Ion Molecule Reactions*; Farrar, J. M., Saunders, W. H., Jr., Eds.; Wiley: New York, 1988; p 61.

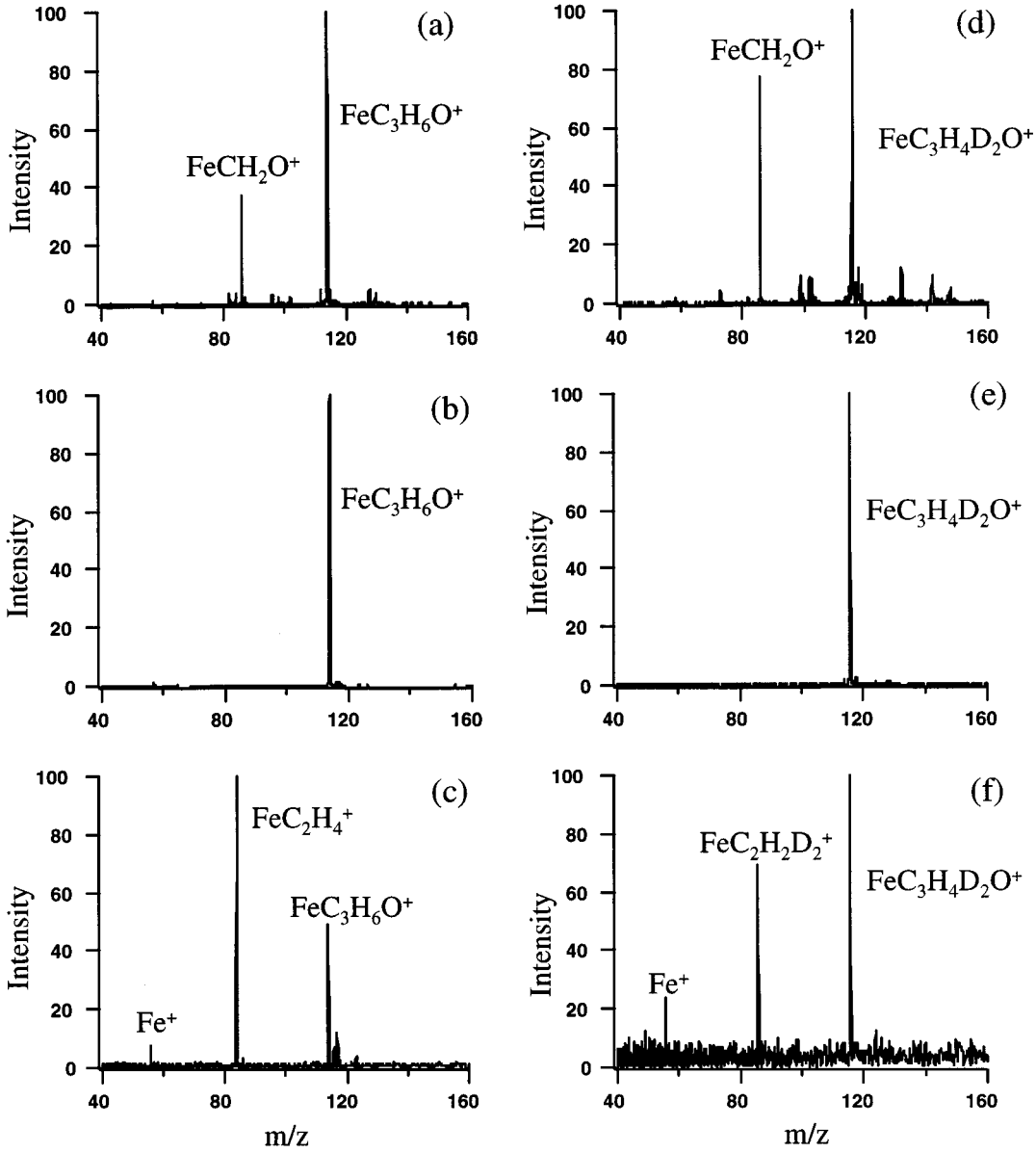


**Figure 1.** (a) Reaction of $Fe(CH_2O)^+$ with propane (400 ms, propane is pulsed into the cell to a maximum pressure of $\sim 1.0 \times 10^{-6}$ Torr); (b) isolation of product ion, $FeC_3H_6O^+$; (c) CID of $FeC_3H_6O^+$; (d) reaction of $Fe(CH_2O)^+$ with [2,2-$D_2$]propane (400 ms, [2,2-$D_2$]propane is pulsed into the cell to a maximum pressure of $\sim 1.0 \times 10^{-6}$ Torr); (e) isolation of product ion, $FeC_3H_4D_2O^+$; and (f) CID of $FeC_3H_4D_2O^+$.

**Scheme 1**

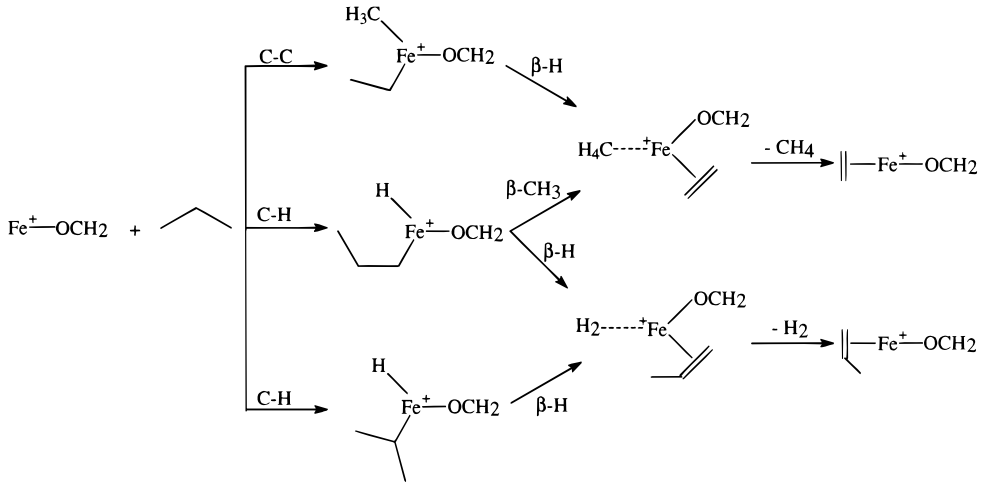


For the kinetics study, the alkane neutrals were introduced into the cell through a Varian leak valve and the reaction time was varied between 200 ms and 2 s. The pressure of the neutral reagent was kept at $\sim 2.5 \times 10^{-7}$ Torr, and Ar was used as the cooling gas at a total pressure of $\sim 1.0 \times 10^{-5}$ Torr. The pressure of the alkane neutral was measured by using standard procedures for calibrating the ion gauge

**Scheme 2**

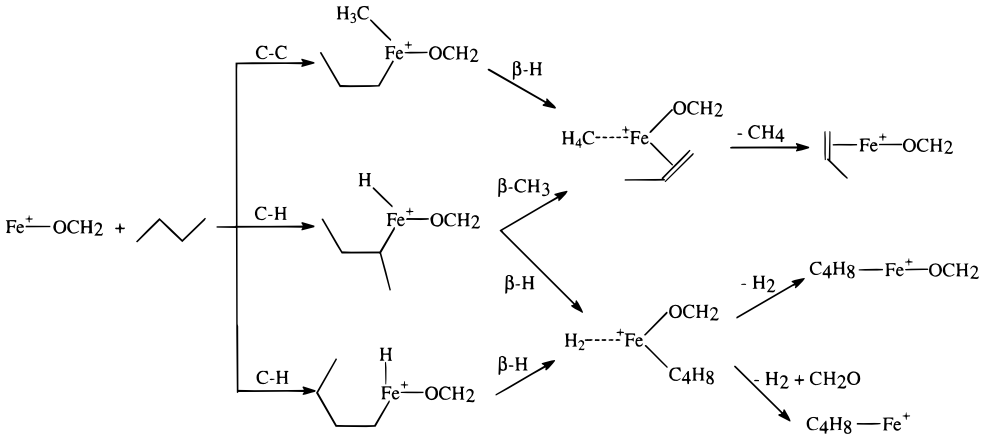


for the sensitivity toward the alkane.[41] The uncertainty in the pressure introduces an error of ±30% into the measurement of the absolute reaction rate constants, while the relative reaction rate constants are more reliable. The branching ratios of primary product ions are reproducible to within ±10% absolute.

## Computations

Theoretical calculations were carried out first at the Hartree−Fock level for full geometry optimization of $Fe(CH_2O)^+$, $Fe(CH_2S)^+$, $CH_2O$, and $CH_2S$, using the effective core potential derived by Hay and Wadt[42] for Fe and the Dunning−Hay double-ζ basis set for C, H, O, and S atoms.[43] To treat the effect of electron correlation, all calculations were repeated by using DFT with Becke-3-LYP for the exchange correlation functional.[44] This functional has three fitted parameters and includes the Hartree−Fock exchange term. Of course this functional is not exact,[45] but gives relatively accurate results for bond dissociation energies and geometries of transition metal compounds.[46] The final calculations with Becke-3-LYP were carried out with the 6-311+G* basis set for C, H, O, and S atoms and the Wachters−Hay all-electron basis set for Fe,[47] resulting in a (611111111|51111|311) [9s 5p 3d] contraction. Corrections for zero-point energy have been taken into account, as well as different spin configurations for $Fe^+$ including $^4F$ and $^6D$ states. All of the calculations were performed with the Gaussian 94 program package[48] at the Purdue University Computer Center (PUCC) and on a Silicon Graphics O2 workstation in our laboratory.

## Results and Discussion

The structures of $Fe(CH_2O)^+$ and $Fe(CH_2S)^+$ ions were studied qualitatively by collision-induced dissociation. Loss of the ligands, $CH_2O$ and $CH_2S$, respectively, to regenerate $Fe^+$ is the only fragmentation process observed in the CID spectra over the energy range studied (∼10−200 eV laboratory frame), strongly suggesting that both $CH_2O$ and $CH_2S$ remain intact when coordinated to $Fe^+$. These results are supported by ligand displacement reactions and the theoretical calculations, as discussed below.

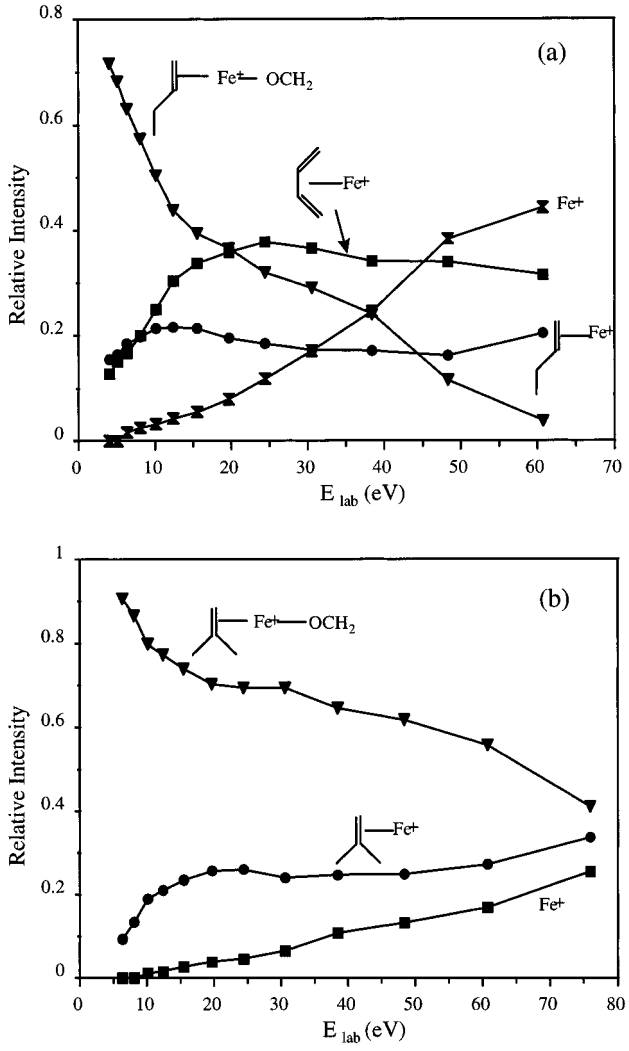


**Figure 2.** Energy-resolved CID plots of two $FeC_5H_{10}O^+$ isomers: (a) $CH_2O$−$Fe^+$−1-butene and (b) $CH_2O$−$Fe^+$−2-methylpropene.

**1. The Reactions of $Fe(CH_2O)^+$ with Linear and Branched Alkanes.** The primary products for the reactions of $Fe(CH_2O)^+$ with selected linear and branched alkanes are presented in Table

(41) Bartmess, J. E.; Georgiadis, R. M. *Vacuum* **1983**, *33*, 149.
(42) Hay, P. J.; Wadt, W. R. *J. Chem. Phys.* **1985**, *82*, 299.
(43) Dunning, T. H., Jr.; Hay, P. J. In *Modern Theoretical Chemistry*; Schaefer, H. F., III, Ed.; Plenum: New York, 1976.
(44) (a) Becke, A. D. *Phys. Rev.* **1988**, *A38*, 3098. (b) Becke, A. D. *J. Chem. Phys.* **1993**, *98*, 1372. (c) Becke, A. D. *J. Chem. Phys.* **1993**, *98*, 5648. (d) Stephens, P. J.; Devlin, F. J.; Chabalowski, C. F.; Frisch, M. J. *J. Phys. Chem.* **1994**, *98*, 11623.
(45) Kais, S.; Herschbach, N. C. H.; Murray, C. W.; Lamimg, G. J. *J. Chem. Phys.* **1993**, *99*, 417.
(46) Siegbahn, P. E. M. *Adv. Chem. Phys.* **1996**, *93*, 333.
(47) (a) Wachters, A. J. H. *J. Chem. Phys.*, **1970**, *52*, 103. (b) Hay, P. J. *J. Chem. Phys.* **1977**, *66*, 4377.
(48) Frisch, M. J.; Trucks, G. W.; Schlegel, H. B.; Gill, P. M. W.; Johnson, B. G.; Robb, M. A.; Cheeseman, J. R.; Keith, T. A.; Petersson, G. A.; Montgomery, J. A.; Raghavachari, K.; Al-Laham, M. A.; Zakrzewski, V. G.; Ortiz, J. V.; Foresman, J. B.; Cioslowski, J.; Stefanov, B. B.; Nanayakkara, A.; Challacombe, M.; Peng, C. W.; Ayala, P. Y.; Chen, W.; Wong, M. W.; Anfres, J. L.; Replogle, E. S.; Gomperts, R.; Martin, R. L.; Fox, D. J.; Binkley, J. S.; Defrees, D. J.; Baker, J.; Stewart, J. P.; Head-Gordon, M.; Gonzalez, C.; Pople, J. A. *Gaussian 94* (Revision D.1); Gaussian, Inc.: Pittsburgh, PA, 1995.

**Table 2.** Fragment Ions Observed from CID on the Major $FeC_nH_{2n}O^+$ Product Ions from $Fe(CH_2O)^+$ Reactions

| | | Fragment Ions | | | | | | |
|---|---|---|---|---|---|---|---|---|
| $FeC_nH_{2n}O^+$ | Structure |  |  | 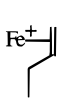 |  |  | 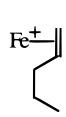 | $Fe^+$ |
| $FeC_3H_6O^+$ |  | X | | | | | | X |
| $FeC_4H_8O^+$ |  | | X | | | | | X |
| $FeC_5H_{10}O^+$ | 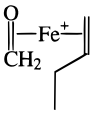 | | | X | X | | | X |
| $FeC_5H_{10}O^+$ | 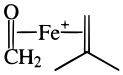 | | | | | X | | X |
| $FeC_6H_{12}O^+$ | 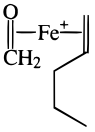 | | X | | | | X | X |

1. $Fe(CH_2O)^+$ reacts in a similar fashion to $Fe^+$, with oxidative insertion of the metal into C−C bonds predominating and less than 10% of the products arising from dehydrogenation. Like $Fe^+$,[49] $Fe(CH_2O)^+$ is unreactive with methane and ethane, but does react with propane. The predominant product generated is $FeC_3H_6O^+$ from $CH_4$ loss, and the minor product is $FeC_4H_8O^+$, formed by dehydrogenation. A mechanism is proposed in Scheme 1, which is analogous to that for $Fe^+$, in which initial oxidative insertion is followed by reductive elimination of an alkane or $H_2$. CID of the product ion, $FeC_3H_6O^+$, yields $FeC_2H_4^+$ via loss of $CH_2O$ as the major fragment and $Fe(CH_2O)^+$ via loss of $C_2H_4$ as the minor fragment at low collision energies, while at higher collision energies loss of $CH_2O + C_2H_4$ is observed. These results are consistent with the CID study of $[Fe, C_3, H_6, O]^+$ isomers by Schwarz and co-workers.[50a] The reaction of $FeC_3H_6O^+$ with acetonitrile yields sequential displacements of $CH_2O$ and $C_2H_4$, reaction 3. These results strongly support the $Fe(C_2H_4)(CH_2O)^+$ structure of the product ion proposed in Scheme 1.

$$Fe(CH_2O)(C_2H_4)^+ \xrightarrow{CH_3CN} Fe(C_2H_4)(CH_3CN)^+ \xrightarrow{CH_3CN} Fe(CH_3CN)_2^+ \quad (3)$$

To further investigate the mechanism, [2,2-$D_2$]propane was reacted with $Fe(CH_2O)^+$, Figure 1. The only primary product ion observed was $FeC_3H_4D_2O^+$, formed from the loss of $CH_4$. Furthermore, CID of $FeC_3H_4D_2O^+$ clearly yields $FeC_2H_2D_2^+$ and $Fe^+$, via loss of $CH_2O$ and $CH_2O + C_2H_2D_2$, respectively. These results support the C−C insertion mechanism for $Fe(CH_2O)^+$, depicted in Scheme 1, and indicate the absence of scrambling. It is evident that $CH_2O$ is a spectator ligand and does not participate in any rearrangement during the reaction. Finally, these results suggest that $D^0(Fe^+-CH_2O) < D^0(Fe^+-C_2H_4) = 34 \pm 2$ kcal/mol,[51] which is in accordance with $D^0(Fe^+-CH_2O) = 33.4 \pm 1.7$ kcal/mol, obtained by Schwarz and co-workers[31] using the kinetic method,[52,53] and $33.0 \pm 1.6$ kcal/mol reported by Tjelta and Armentrout with the guided ion beam experiment.[32]

The reaction of $Fe(CH_2O)^+$ with *n*-butane is also dominated by $CH_4$ loss, yielding $FeC_4H_8O^+$ as the predominant product. Interestingly, some $Fe(butene)^+$ was also observed, which apparently results from initial C−H insertion, followed by $\beta$-hydrogen transfer and then $H_2 + CH_2O$ loss. This reaction pathway competes with simple $H_2$ loss and is illustrated in Scheme 2. CID of $FeC_4H_8O^+$ readily produces $Fe(propene)^+$, in accordance with the predicted $CH_2O-Fe^+-$propene structure.

The reaction with *n*-pentane is similar to that with *n*-butane. CID of the major product, $FeC_5H_{10}O^+$, yields $Fe(butene)^+$, $Fe(butadiene)^+$, and $Fe^+$, which again is consistent with the $CH_2O-Fe^+-$butene complex predicted. Further CID of $Fe(butene)^+$ gives $Fe(butadiene)^+$ and $Fe^+$ with neutral loss of $H_2$ and $C_4H_8$, respectively. These results are consistent with a linear butene ligand[4] and will be compared with the 2-methylpropene isomer below.

The reactions of $Fe(CH_2O)^+$ with 2-methylpropane and 2-methylbutane continue the trend with terminal C−C insertion preferred, leading to $CH_4$ loss. Less than 10% of the product ions result from dehydrogenation. $Fe(CH_2O)^+$ reacts with 2,2-dimethylpropane to eliminate $CH_4$, giving $CH_2O-Fe^+-C_4H_8$, exclusively. No dehydrogenation is observed since there are no $\beta$ hydrogens available to transfer, making reductive elimination of $H_2$ impossible. CID of the $CH_2O-Fe^+-C_4H_8$ product ion produces $FeC_4H_8^+$ and $Fe^+$. Further CID of $FeC_4H_8^+$ gives

(49) Byrd, G. D.; Burnier, R. C.; Freiser, B. S. *J. Am. Chem. Soc.* **1982**, *104*, 3565.
(50) Schwarz, J.; Wesendrup, R.; Schröder, D.; Schwarz, H. *Chem. Ber.* **1996**, *129*, 1463.
(51) Jacobson, D. B.; Freiser, B. S. *J. Am. Chem. Soc.* **1983**, *105*, 7492.
(52) McLuckey, S. A.; Schoen, A. E.; Cooks, R. G. *J. Am. Chem. Soc.* **1982**, *104*, 848.
(53) Cooks, R. G.; Pattrick, J. S.; Kotiaho, T.; McLuckey, S. A. *Mass Spectrom. Rev.* **1994**, *13*, 287.

$Fe^+$ as the only fragment, indicative of Fe(2-methylpropene)$^+$. Thus, the $FeC_5H_{10}O^+$ from 2,2-dimethylpropane, $CH_2O-Fe^+-$2-methyl-propene, is an isomer of the product ion from *n*-pentane. The two isomers are clearly differentiated by collision-induced dissociation, as shown by a comparison of CID plots in Figure 2. Also, Table 2 summarizes all of the CID results.

It is interesting that terminal C−C insertion, resulting in $CH_4$ loss, is the preferred insertion mode for the above reactions, even though the terminal C−C bond is the strongest in the chain. This is in contrast to the reactions of bare $Fe^+$ with alkanes in which terminal C−C insertion is the least preferred attack mode and central C−C bond cleavage, resulting in larger alkane loss, is favored.[49] One explanation is that with the $CH_2O$ ligand on $Fe^+$, central C−C insertion is more sterically hindered, but additional factors are discussed below.

Starting with *n*-hexane and *n*-heptane, the reactivity trend changes in that not only is $C_2H_6$ loss observed, but it is more prevalent than $CH_4$ loss. CID of $FeC_5H_{10}O^+$, obtained from the hexane reaction by $C_2H_6$ loss, yields the same results as the $FeC_5H_{10}O^+$ product generated from the pentane reaction, indicative of a $CH_2O-Fe^+-$butene complex. Multimembered-ring intermediates have been proposed by Armentrout and co-workers[54] and Schwarz and co-workers[29] to explain the gas-phase reactions of $Fe^+$ with small alkanes. In our study, the five-membered-ring intermediate **1** could lead to $C_2H_6$ loss in the hexane reaction, while the six-membered-ring intermediate **2** could then eliminate $CH_4$. Similarly, for the heptane reaction, loss of $C_2H_6$ would involve a six-membered-ring intermediate(**3**).

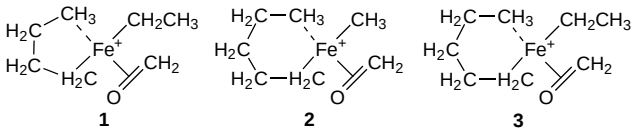


To further test these proposed intermediates, *n*-octane, *n*-nonane, and *n*-decane were reacted with Fe$(CH_2O)^+$. As summarized in Table 1, both octane and nonane react with Fe$(CH_2O)^+$ to yield $C_2H_6$ loss, while, surprisingly, the reaction with decane results predominantly in $C_4H_{10}$ loss. Once again, after terminal C−C insertion, the alkyl chain can fold back to stabilize the metal ion forming multimembered-ring intermediates.[25] However, it is evident that this alkyl chain stabilization effect is not the only determining factor and the exact mechanism remains elusive.

**2. The Reactions of Fe$(CH_2S)^+$ with Linear and Branched Alkanes.** In contrast to Fe$(CH_2O)^+$, the reactions of Fe$(CH_2S)^+$ with alkanes resemble more those of other ligated species, such as $FeS^+$, $FeO^+$, $FeCH_2^+$, and so forth, which react mainly by initial C−H insertion.[13−20] The distributions of primary products for the reactions of Fe$(CH_2S)^+$ with linear and branched alkanes are given in Table 3. Elimination of $H_2S$ is observed for each of the alkanes studied, either as a major or a minor product, and can be explained by a sequence involving initial C−H oxidative insertion, hydrogen transfer to sulfur, followed by a migratory insertion of methylene into the metal−alkyl bond. This results in the formation of an activated $H_2S-Fe^+-$olefin complex, which then dissociates by the elimination of $H_2S$ (see Scheme 3). Products resulting from initial C−C insertion, followed by small alkane or alkene loss, are also observed.

(54) (a) Haynes, C. L.; Chen, Y.-M.; Armentrout, P. B. *J. Phys. Chem.* **1995**, *99*, 9110. (b) Haynes, C. L.; Chen, Y.-M.; Armentrout, P. B. *J. Phys. Chem.* **1996**, *100*, 111.

**Table 3.** Product Distributions for the Reactions of Fe$(CH_2S)^+$ with Linear and Branched Alkanes

| | products | | |
|---|---|---|---|
| alkane | ion | ion percentage | neutral loss |
| methane | no reaction | | |
| ethane | $FeC_3H_6^+$ | 33 | $H_2S$ |
| | $FeC_3H_4S^+$ | 67 | $C_2H_4$ |
| propane | $FeC_4H_8^+$ | 100 | $H_2S$ |
| [2,2-$D_2$]propane | $FeC_4H_6D_2^+$ | 65 | $H_2S$ |
| | $FeC_4H_7D^+$ | 32 | HDS |
| | $FeC_4H_8^+$ | 3 | $D_2S$ |
| *n*-butane | $FeC_5H_{10}^+$ | 53 | $H_2S$ |
| | $FeC_4H_8S^+$ | 22 | $CH_4$ |
| | $FeC_3H_8S^+$ | 10 | $C_2H_4$ |
| | $FeC_4H_8^+$ | 7 | $CH_3SH$ |
| | $FeC_5H_{10}S^+$ | 5 | $H_2$ |
| | $FeC_4H_6^+$ | 3 | $CH_2S$, $2H_2$ |
| *n*-pentane | $FeC_5H_{10}S^+$ | 28 | $CH_4$ |
| | $FeC_4H_{10}S^+$ | 22 | $C_2H_4$ |
| | $FeC_6H_{12}^+$ | 20 | $H_2S$ |
| | $FeC_5H_{10}^+$ | 15 | $CH_3SH$ |
| | $FeC_3H_8S^+$ | 8 | $C_3H_6$ |
| | $FeC_5H_8^+$ | 7 | $CH_2S$, $2H_2$ |
| 2-methylpropane | $FeC_5H_{10}^+$ | 55 | $H_2S$ |
| | $FeC_4H_8S^+$ | 29 | $CH_4$ |
| | $FeC_5H_{10}S^+$ | 8 | $H_2$ |
| | $FeC_4H_8^+$ | 8 | $CH_3SH$ |
| 2,2-dimethylpropane | $FeC_5H_{10}S^+$ | 91 | $CH_4$ |
| | $FeC_6H_{12}^+$ | 5 | $H_2S$ |
| | $FeC_5H_8^+$ | 4 | $CH_2S$, $2H_2$ |
| 2-methylbutane | $FeC_5H_{10}S^+$ | 53 | $CH_4$ |
| | $FeC_6H_{12}^+$ | 17 | $H_2S$ |
| | $FeC_5H_8^+$ | 10 | $CH_2S$, $2H_2$ |
| | $FeC_4H_{10}S^+$ | 8 | $C_2H_4$ |
| | $FeC_6H_{12}S^+$ | 5 | $H_2$ |
| | $FeC_3H_8S^+$ | 4 | $C_3H_6$ |
| | $FeC_5H_{10}^+$ | 3 | $CH_3SH$ |
| *n*-hexane | $FeC_6H_{12}^+$ | 54 | $CH_3SH$ |
| | $FeC_4H_{10}S^+$ | 16 | $C_3H_6$ |
| | $FeC_5H_{12}S^+$ | 16 | $C_2H_4$ |
| | $FeC_7H_{14}^+$ | 7 | $H_2S$ |
| | $FeC_6H_{12}S^+$ | 7 | $CH_4$ |

Fe$(CH_2S)^+$ is unreactive with methane, as are $Fe^+$ and Fe$(CH_2O)^+$. While both $Fe^+$ and Fe$(CH_2O)^+$ fail to react with ethane, however, Fe$(CH_2S)^+$ reacts slowly to produce Fe(propene)$^+$ and Fe$(CH_3SH)^+$ by $H_2S$ loss and $C_2H_4$ loss, respectively. These reactions imply $D^0(Fe^+-H_2S) < D^0(Fe^+-C_3H_6) = 37 \pm 2$ kcal/mol [51] and $D^0(Fe^+-CH_3SH) > D^0(Fe^+-C_2H_4) = 34 \pm 2$ kcal/mol.[51] Reaction with propane yields $FeC_4H_8^+$, exclusively, via $H_2S$ loss. CID of the $FeC_4H_8^+$ product yields $FeC_4H_6^+$ and $Fe^+$, which is consistent with Fe(butene)$^+$.[4] In addition, reaction of Fe$(CH_2S)^+$ with [2,2-$D_2$]propane leads to complete scrambling in the $H_2S$ loss isotopologs. The experimental results are in excellent agreement with the predicted statistical distribution of 62%, 36%, and 2% for loss of $H_2S$, HDS, and $D_2S$, respectively. A mechanism for scrambling involving both terminal C−H insertion and central C−D insertion is given in Schemes 4 and 5. Figure 3 shows the reactions of Fe$(CH_2S)^+$ with propane and [2,2-$D_2$]propane. Unfortunately, CID of the $FeC_4H_6D_2^+$ product from [2,2-$D_2$]-propane proved unsuccessful, due to the difficulty in obtaining good isolation. To further confirm the proposed total scrambling mechanism, dimethyl-$d_6$ sulfide was used to generate $FeCD_2S^+$. The reaction of $FeCD_2S^+$ with propane yielded 68% $FeC_4D_2H_6^+$, 30% $FeC_4DH_7^+$, and 2% $FeC_4H_8^+$, which once again is in accordance with the above predicted statistical losses of $H_2S$, HDS, and $D_2S$.

The reaction of Fe$(CH_2S)^+$ with *n*-butane is dominated by $H_2S$ loss. CID of the major product, $FeC_5H_{10}^+$, yields Fe(propene)$^+$, Fe(butadiene)$^+$, Fe(ethene)$^+$, and $Fe^+$, indicative

**Scheme 3**

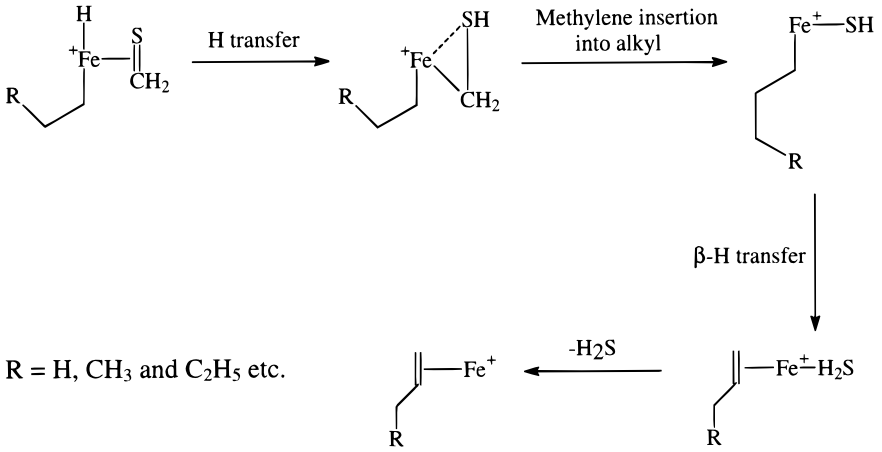


**Scheme 4**

Terminal C-H insertion

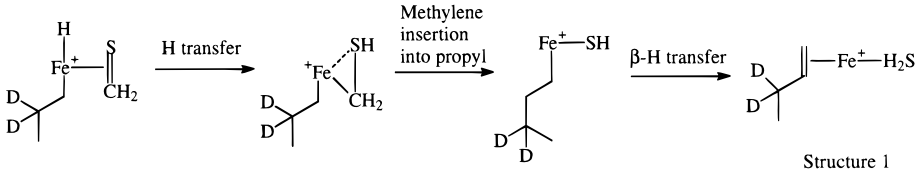


Scrambling starting from structure 1:

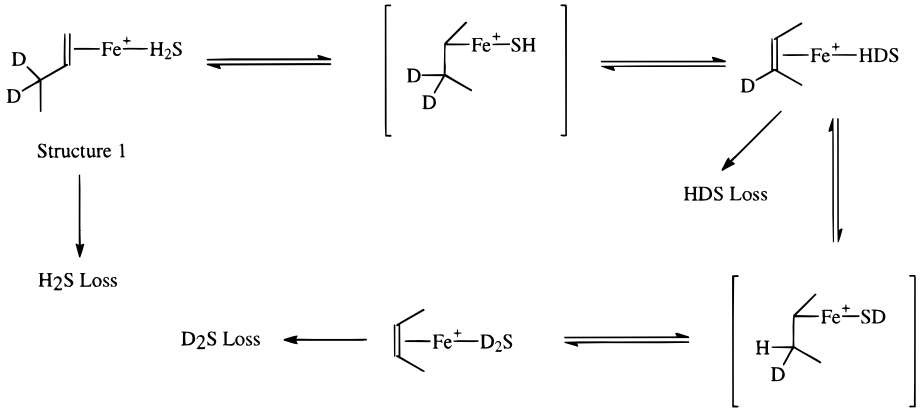


of Fe(pentene)$^+$.[4,55] Interestingly, CID of the second most abundant product ion, $FeC_4H_8S^+$, gives $FeC_4H_6^+$ by $H_2S$ loss as the major fragment, followed by $Fe^+$, Fe(propene)$^+$, and a trace of $Fe(CH_2S)^+$ as the minor fragments. Thus, in this case, rearrangement involving the $CH_2S$ ligand to form $H_2S$ occurs again. A mechanism involving a five-membered metallacyclic intermediate, as shown in Scheme 6, is proposed. An activated $H_2S-Fe^+-C_4H_6$ complex is formed by $\beta$-H transfer, which gives $FeC_4H_6^+$ as the major fragment upon CID. $FeC_4H_8S^+$ was also synthesized directly by a condensation reaction of Fe$(CH_2S)^+$ with propene. CID of this $FeC_4H_8S^+$ yields the same results as that of $FeC_4H_8S^+$ from the reaction of $FeCH_2S^+$ with *n*-butane. The structure of $FeC_4H_8S^+$ was further probed by reacting it with benzene, resulting in a sequential displacement of $H_2S$ and $C_4H_6$, reaction 4. All of these results strongly support the above rearrangement mechanism. The minor CID product of $FeC_4H_8S^+$ is $Fe(CH_2S)^+$, which suggests that $D^0(Fe^+-CH_2S) > D^0(Fe^+-C_3H_6) = 37 \pm 2$ kcal/mol.[51]

$$Fe(CH_2S)(C_3H_6)^+ \xrightarrow{\text{rearrangement}} C_4H_6-Fe^+-H_2S \xrightarrow{C_6H_6} Fe(C_4H_6)(C_6H_6)^+ \xrightarrow{C_6H_6} Fe(C_6H_6)_2^+ \quad (4)$$

The reaction of $Fe(CH_2S)^+$ with *n*-pentane is, once again, dominated by $H_2S$ loss, arising from C−H insertion and $CH_4$ loss from C−C insertion. CID of one of the major product ions, $FeC_5H_{10}S^+$, gives $FeC_5H_8^+$, presumably Fe(2-methylbutadiene)$^+$, and $Fe^+$, via $H_2S$ and $H_2S + C_5H_8$ loss, respectively. Furthermore, reaction of $FeC_5H_{10}S^+$ with benzene yields sequential displacements of $H_2S$ and $C_5H_8$, reaction 5. $FeC_5H_{10}S^+$, generated by an alternative synthetic route, the reaction of $Fe(CH_2S)^+$ with pulsed-in 1-butene, gives the same results. Hence, formation of an $H_2S-Fe^+-C_5H_8$ complex is common in both reaction routes. This again supports the proposed rearrangement mechanism.

$$Fe(CH_2S)(C_4H_8)^+ \xrightarrow{\text{rearrangement}} C_5H_8-Fe^+-H_2S \xrightarrow{C_6H_6} Fe(C_5H_8)(C_6H_6)^+ \xrightarrow{C_6H_6} Fe(C_6H_6)_2^+ \quad (5)$$

(55) Wesendrup, R.; Schalley, C. A.; Schröder, D.; Schwarz, H. *Organometallics* **1996**, *15*, 1435.

**Scheme 5**

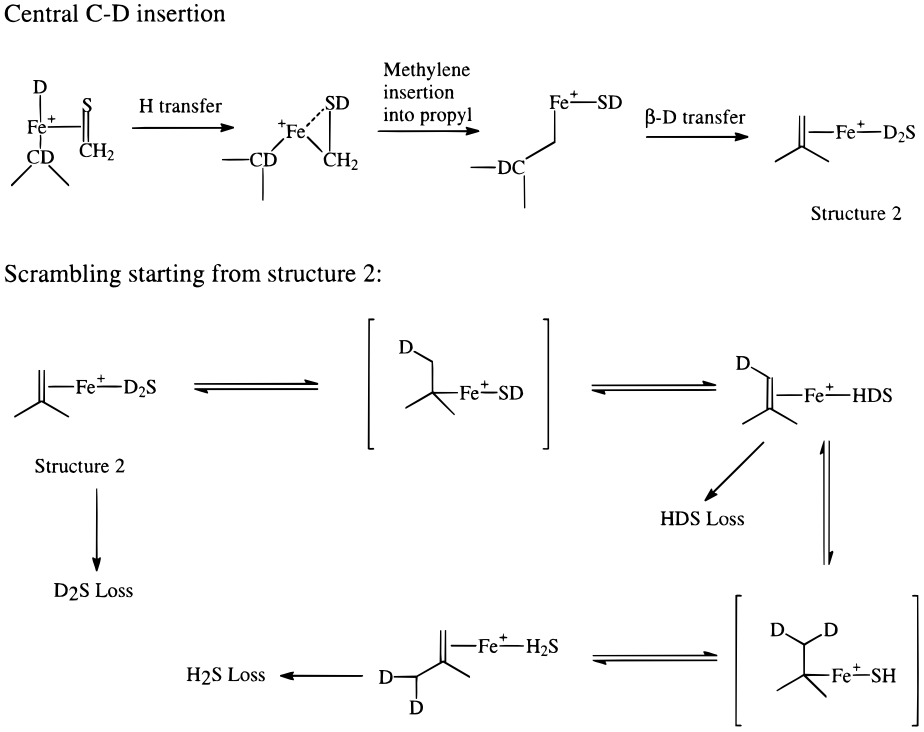


The reaction of $Fe(CH_2S)^+$ with *n*-hexane is somewhat different. The major product ion is $FeC_6H_{12}^+$ formed, after initial C−H insertion, by loss of $CH_3SH$. CID of $FeC_6H_{12}^+$ gives $FeC_4H_8^+$ and $FeC_4H_6^+$ by neutral loss of $C_2H_4$ and $C_2H_6$, respectively, which are consistent with an $Fe(hexene)^+$ structure.[4] Apparently, in this case, the methylene insertion step proposed in our mechanism is hindered by the bulky alkyl chain and, hence, instead of methylene insertion, intact $CH_3SH$ loss occurs.

The reaction with 2-methylpropane is similar to that of *n*-butane, with $H_2S$ loss as the dominant process. CID of the major product ion, $FeC_5H_{10}^+$, generates the same fragments as the $FeC_5H_{10}^+$ from the *n*-butane reaction. As for the reaction with 2,2-dimethylpropane, terminal C−C insertion is dominant, since no $\beta$ hydrogens are available subsequent to initial C−H insertion. The major product ion, $FeC_5H_{10}S^+$, yields $FeC_5H_8^+$ and $Fe^+$ upon collision-induced dissociation. These results are indicative of an $H_2S-Fe^+-C_5H_8$ complex, which can be formed through a five-membered metallacyclic intermediate. The reaction of $Fe(CH_2S)^+$ with 2-methylbutane resembles the reaction of *n*-pentane, with C−H insertion followed by $H_2S$ loss. CID of $FeC_5H_{10}S^+$, which results from $CH_4$ loss, gives $Fe(C_5H_8)^+$ and $Fe^+$. The CID results of $FeC_nH_{2n}^+$ types of ions are summarized in Table 4.

Finally, reaction of $Fe(CH_2S)^+$ with pulsed-in benzene yields $Fe(benzene)^+$, exclusively. This result, in conjunction with the CID results discussed above, yields the bracket $D^0(Fe^+-C_3H_6) = 37 \pm 2$ kcal/mol $< D^0(Fe^+-CH_2S) < D^0(Fe^+-C_6H_6) = 49.6 \pm 2.3$ kcal/mol.[56] Unfortunately, determination of the bond energies of both $Fe(CH_2O)^+$ and $Fe(CH_2S)^+$ by photodissociation methods[57] failed, since neither $Fe(CH_2O)^+$ nor $Fe(CH_2S)^+$ was observed to dissociate upon irradiation in the visible region.

**3. Kinetics Studies with Selected Alkanes.** Pseudo-first-order kinetics are observed for the reactions of $Fe(CH_2O)^+$ and $Fe(CH_2S)^+$ with propane and *n*-pentane, respectively. For example, the kinetics plots for the reactions of $Fe(CH_2O)^+$ and $Fe(CH_2S)^+$ with propane are shown in Figure 4. [*A*] is the reactant ion intensity after time *t*, and [$A_0$] is obtained by summing the intensities of the reactant ion and product ions at each time. The slopes of the pseudo-first-order plots are used with the calibrated reactant pressure to obtain the observed rate constants, $k_{ob}$. The estimated rate constants with propane are $8.0 \times 10^{-12}$ and $6.6 \times 10^{-12}$ cm$^3$ molecule$^{-1}$ s$^{-1}$ for $Fe(CH_2O)^+$ and $Fe(CH_2S)^+$, respectively. These reactions are one order of magnitude slower than that of the unligated $Fe^+$.[2] The experimental rate constant for the reaction of $Fe(CH_2O)^+$ with *n*-octane was also obtained to evaluate the reaction trend. These values are given in Table 5 along with the calculated Langevin rate constants, $k_L$, and the reaction efficiencies.[58,59] The linear pseudo-first-order kinetics observed for these reactions suggest that the $Fe(CH_2O)^+$ and $Fe(CH_2S)^+$ species are thermalized and consist of one isomeric structure. A comparison of the reaction efficiencies in this limited study shows that the reactions of $Fe(CH_2O)^+$ are somewhat more efficient than that of $Fe(CH_2S)^+$. In addition, as the length of the alkane chain increases, the reaction efficiencies increase dramatically.

**4. Theoretical Calculations: Geometries and Bonding.** Theoretical studies have contributed significantly to our understanding of the bonding in metal ion systems.[60−67,70−72] In addition they also provide metal ion−ligand binding energies which are generally in good agreement with the experimental

(56) Meyer, F.; Khan, F. A.; Armentrout, P. B. *J. Am. Chem. Soc.* **1995**, *117*, 9740.

(57) (a) Hettich, R. L.; Jackson, T. C.; Stanko, E. M.; Freiser, B. S. *J. Am. Chem. Soc.* **1986**, *108*, 5086. (b) Ranasinghe, Y. A.; Surjasasmita, I. B.; Freiser, B. S. In *Organometallic Ion Chemistry*, Freiser, B. S., Ed.; Kluwer Academic Publishers: Dordrecht, 1996; Chapter 7.

(58) Su, T.; Bowers, M. T. *Int. J. Mass Spectrom. Ion Phys.* **1973**, *12*, 347.

(59) Miller, K. J. *J. Am. Chem. Soc.*, **1990**, *112*, 8533.

(60) Bauschlicher, C. W., Jr.; Langhoff, S. R.; Partridge, H. In *Organometallic Ion Chemistry*; Freiser, B. S., Ed.; Kluwer Academic Publishers: Dordrecht, 1996; Chapter 2.

(61) Sodupe, M.; Bauschlicher, C. W., Jr. *Chem. Phys. Lett.* **1991**, *181*, 321.

(62) Holthausen, M. C.; Koch, W. *Helv. Chim. Acta* **1996**, *79*, 1939.

(63) (a) Bauschlicher, C. W., Jr.; Sodupe, M. *Chem. Phys. Lett.* **1995**, *240*, 526. (b) Xu, Y. C.; Garcia, E.; Freiser, B. S.; Bauschlicher, C. W., Jr. *Int. J. Mass Spectrom. Ion Proc.* **1996**, *157/158*, 249.

(64) Schwarz, J.; Schröder, D.; Schwarz, H.; Heinemann, C.; Hrušák, J. *Helv. Chim. Acta* **1996**, *79*, 1110.

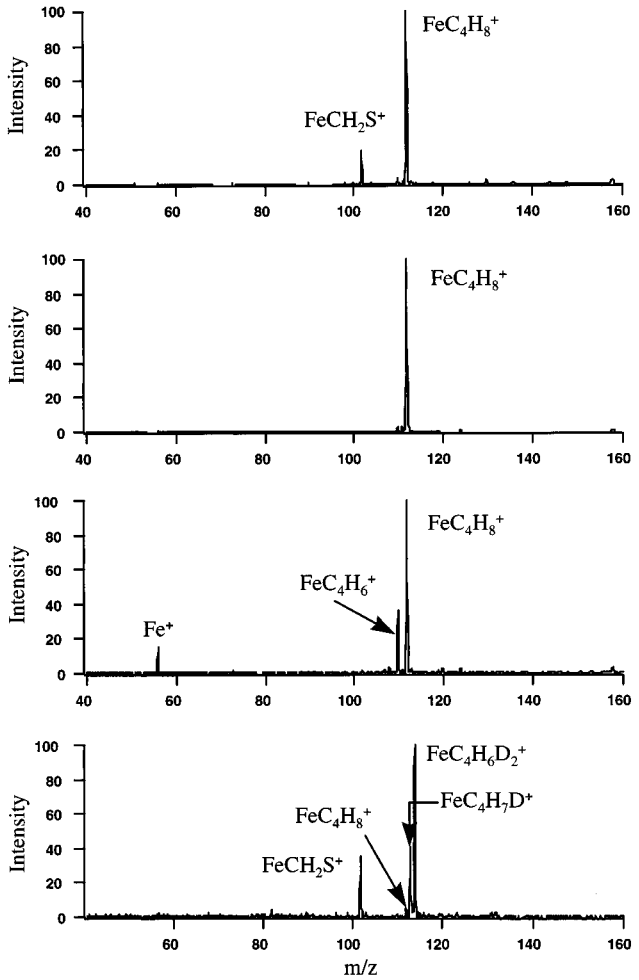


**Figure 3.** (a) Reaction of $Fe(CH_2S)^+$ with propane (400 ms, propane is pulsed into the cell to a maximum pressure of $\sim 1.0 \times 10^{-6}$ Torr); (b) isolation of product ion, $FeC_4H_8^+$; (c) CID of $FeC_4H_8^+$; and (d) reaction of $Fe(CH_2S)^+$ with [2,2-$D_2$]propane (400 ms, [2,2-$D_2$]propane is pulsed into the cell to a maximum pressure of $\sim 1.0 \times 10^{-6}$ Torr).

**Scheme 6**

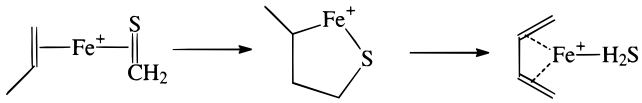


values. To further understand the differences in the reactivities of $Fe(CH_2O)^+$ and $Fe(CH_2S)^+$, density functional calculations were performed to elucidate the metal ion−ligand bonding structures of these two species.

There are two bonding mechanisms that are considered in the $Fe(CH_2O)^+$ and $Fe(CH_2S)^+$ systems. One possibility is that $Fe^+$ binds electrostatically from the $^6D(3d^64s^1)$ ground state.[63]

**Table 4.** Percentage of Neutral Losses from CID of the $FeC_nH_{2n}^+$ Product Ions from the Reactions of $Fe(CH_2S)^+$

| | neutrals lost | | | | | | | |
|---|---|---|---|---|---|---|---|---|
| product ion | $H_2$ | $CH_4$ | $C_2H_4$ | $(C_2H_4 + H_2)$ | $C_3H_6$ | $C_4H_8$ | $C_5H_{10}$ | $C_6H_{12}$ |
| $FeC_4H_8^+$ [a] | 71 | | | | | 29 | | |
| $FeC_5H_{10}^+$ [b] | | 18 | 58 | | 12 | | 12 | |
| $FeC_6H_{12}^+$ [c] | | | 57 | 33 | | | | 10 |

[a] Under 32 eV lab energy. [b] Under 35 eV lab energy. [c] Under 20 eV lab energy.

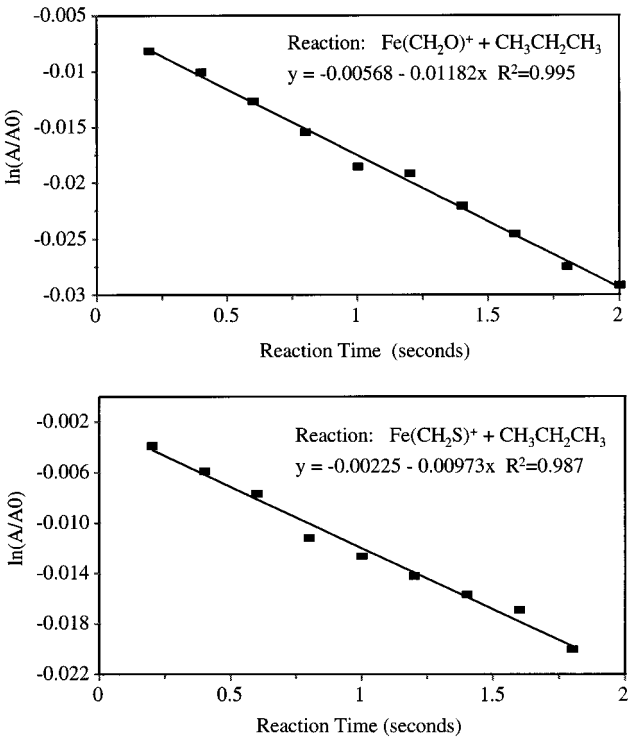


**Figure 4.** Pseudo-first-order plots of the reaction of $Fe(CH_2O)^+$ and $Fe(CH_2S)^+$ with propane leaked into the cell at $\sim 2.5 \times 10^{-7}$ Torr.

**Table 5.** Rate Constants ($cm^3$ $molecule^{-1}$ $s^{-1}$) and Calculated Reaction Efficiencies for the Reactions of $Fe(CH_2O)^+$ and $Fe(CH_2S)^+$ with Selected Alkanes

| reaction | $k_{ob}$ | $k_L$ | reaction eff (%) |
|---|---|---|---|
| $FeCH_2O^+$ + propane | $8.0 \times 10^{-12}$ | $1.1 \times 10^{-9}$ | 0.7 |
| $FeCH_2O^+$ + *n*-pentane | $2.9 \times 10^{-10}$ | $1.2 \times 10^{-9}$ | 25 |
| $FeCH_2O^+$ + *n*-octane | $5.3 \times 10^{-10}$ | $1.3 \times 10^{-9}$ | 40 |
| $FeCH_2S^+$ + propane | $6.6 \times 10^{-12}$ | $1.1 \times 10^{-9}$ | 0.6 |
| $FeCH_2S^+$ + *n*-pentane | $2.1 \times 10^{-10}$ | $1.1 \times 10^{-9}$ | 19 |
| $Fe^+$ + propane[a] | $8.3 \times 10^{-11}$ | $1.1 \times 10^{-9}$ | 7.5 |

[a] Armentrout and Bowers and their co-workers reported[2] that the total cross section of the reaction of $Fe^+$ ($^6D$) with propane is 7.5% of the Langevin collision cross section. So the thermal rate constant was obtained by multiplying $k_L$ with 0.075.

In this case, the 4s orbital of Fe is polarized away from the $CH_2X$ (X = O or S) to reduce the Fe and ligand repulsion and this will lead to sextet ground states. The other bonding mechanism involves the formation of $\pi$ complexes.[63] $Fe^+$ is promoted to the $^4F(3d^7)$ state, since larger 3d occupation will increase the Fe 3d to $\pi^*$ back-donation. It also reduces the Fe−ligand repulsion, since the 3d orbital is more compact than the 4s orbital. These benefits could more than make up for the cost of electron promotion (5.8 kcal/mol as the experimental separation of the two states) and result in a $\pi$ complex with a quartet ground state.

For $Fe(CH_2O)^+$ and $Fe(CH_2S)^+$, we searched the minima for both the quartet and sextet states. We found that the ground

(65) (a) Yeh, C. S.; Byun, Y. G.; Afzaal, S.; Freiser, B. S.; Hay, J. P. *J. Am. Chem. Soc.* **1995**, *117*, 4042. (b) Byun, Y. G.; Kan, S. Z.; Lee, S. A.; Kim, Y. H.; Miletic, M.; Bleil, R. E.; Kais, S.; Freiser, B. S. *J. Phys. Chem.* **1996**, *100*, 6336.

(66) Schilling, J. B.; Beauchamp, J. L.; Goddard, W. A., III *J. Am. Chem. Soc.* **1987**, *109*, 4470.

(67) Ferhati, A.; McMahon, T. B.; Ohanessian, G. *J. Am. Chem. Soc.* **1996**, *118*, 5997.

(68) Geometry of free $CH_2O$ (ground state) with Becke-3-LYP/6-311+G*: $R$(C−O) = 1.201 Å, $R$(C−H) = 1.108 Å, ∠O−C−H = 121.9°.

(69) Geometry of free $CH_2S$ (ground state) with Becke-3-LYP/6-311+G*: $R$(C−S) = 1.615 Å, $R$(C−H) = 1.090 Å, ∠S−C−H = 122.2°.

(70) Fiedler, A.; Schröder, D.; Schwarz, H.; Tjelta, B. L.; Armentrout, P. B. *J. Am. Chem. Soc.* **1996**, *118*, 5047.

(71) Fisher, E. R.; Armentrout, P. B. *J. Phys. Chem.* **1990**, *94*, 1674.

(72) Bauschlicher, C. W., Jr.; Partridge, H. *J. Phys. Chem.* **1991**, *95*, 3946.

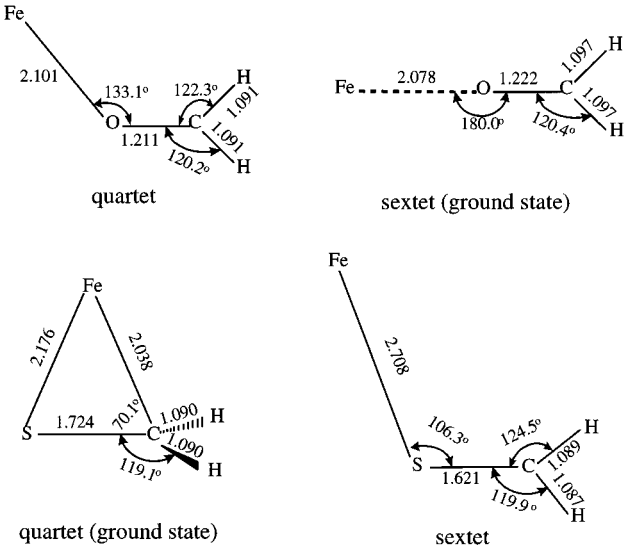


**Figure 5.** Optimized geometries of sextet and quartet states for both $Fe(CH_2O)^+$ and $Fe(CH_2S)^+$ with Becke-3-LYP, using 6-311+G* for C, H, O, and S, and the Wachters-Hay all electron basis set for Fe with the scaling factors of Raghavachari and Trucks. All distances are given in Å.

state for $Fe(CH_2O)^+$ is the sextet state, which is 0.0236 hartree below the quartet state in our final DFT calculations using 6-311+G* for C, H, O, and S and the Wachters-Hay all-electron basis set for Fe.[47] For $Fe(CH_2S)^+$, the ground state is the quartet state lying 0.0342 hartree below the sextet state. The optimized structures with use of Becke-3-LYP for both ligated metal ions with different spin states are shown in Figure 5. Spin contaminations were small in all of the calculations, and the deviations of $\langle S^2 \rangle$ from the exact values are less than 1%. The binding energies for $Fe(CH_2O)^+$ and $Fe(CH_2S)^+$ were obtained by comparing the total energy for $FeCH_2X^+$ (X = O or S) with the energies of $CH_2X$ and $Fe^+$.

The optimized structure of ground state $Fe(CH_2O)^+$ ($^6A'$) has a planar $C_{2v}$ symmetry with an $R$(Fe−O) distance of 2.078 Å and $R$(C−O) distance of 1.222 Å, which is close to the C═O double bond length of 1.201 Å for the free $CH_2O$ molecule.[68] Thus, the $CH_2O$ unit remains nearly undisturbed compared to the uncomplexed formaldehyde molecule. In this case, $Fe^+$ binds to the oxygen atom of $CH_2O$ predominantly by electrostatic bonding. The binding energy of $Fe^+-CH_2O$ is calculated at 32.2 kcal/mol, which is in excellent agreement with the experimentally determined values of 33.4 ± 1.7 kcal/mol by Schwarz and co-workers[31] and 33.0 ± 1.6 kcal/mol by Tjelta and Armentrout,[32] as well as with our bracketed bond energy of $D^0(Fe^+-CH_2O) < D^0(Fe^+-C_2H_4) = 34 \pm 2$ kcal/mol. Interestingly, recent experimental and theoretical work by Armentrout and co-workers has shown that $HFe^+-OCH_2$ has $C_{2v}$ symmetry with a short Fe−H bond of 1.57 Å and a Fe−O distance of 2.00 Å, while the $CH_2O$ subunit is undisturbed, similar to our calculations.[70] The binding energy of $HFe^+-OCH_2$ is computed as 47 kcal/mol, which is larger than the experimental value of 28 ± 3 kcal/mol. In addition, Fisher and Armentrout have determined that $D^0(Cu^+-CH_2O) = 50.5 \pm 2.5$ kcal/mol from the reaction of $Cu^+$ with ethylene oxide by using the guided ion beam instrument.[71] Bauschlicher *et al.* have shown that $Al(CH_2O)^+$ has $C_{2v}$ symmetry, with the $Al^+$ 1.976 Å away from the oxygen in the plane.[60] They calculated $D^0(Al^+-CH_2O) = 27.2$ kcal/mol for the predominantly electrostatic bond. Similar results were obtained from calculations on $Mg(CH_2O)^+$, with a binding energy of $Mg^+$ to $CH_2O$ of 32.8 kcal/mol.[72] Likewise, our calculations indicate primarily electrostatic bonding between $Fe^+$ and $CH_2O$. The optimized quartet state of $Fe(CH_2O)^+$ ($^4A'$) has planar $C_s$ symmetry, as shown in Figure 5, and lies about 14.8 kcal/mol above the sextet state. The calculated $R$(Fe−O) distance is 2.101 Å, and the angle of Fe−O−C is found to be 133.1°. The $CH_2O$ subunit is almost undisturbed compared to uncomplexed $CH_2O$ with similar bond lengths and bond angles.[68]

The optimized ground state of $Fe(CH_2S)^+$ (quartet) is found to have $C_s$ symmetry with an Fe−S distance of 2.176 Å and an Fe−C distance of 2.038 Å, as shown in Figure 5. The angle of Fe−C−S is 70.1°, and the calculated $R$(C−S) at 1.724 Å is between the C═S double bond length of 1.615 Å[69] and the C−S single bond length of 1.82 Å. The bond between Fe and S is clearly covalent, with a pair of electrons from the sulfur atom donating to the 3d orbital of Fe, while 3d electrons from Fe can back-donate to the $\pi^*$ molecular orbital of thioformaldehyde. The calculated $D^0(Fe^+-CH_2S)$ is 41.5 kcal/mol, which is in accordance with the experimentally obtained bond energy range of 37 ± 2 to 49.6 ± 2.3 kcal/mol. The sextet state $Fe(CH_2S)^+$, a slightly distorted planar $C_s$ structure, is less stable than the quartet state by about 21.5 kcal/mol. The $R$(Fe−S) is elongated to 2.708 Å, compared to 2.176 Å in the quartet state. The $CH_2S$ unit is only slightly disturbed, suggesting that the 4s orbital of Fe binds to the 3p orbital of S.

In the extensive review of the spectroscopy of formaldehyde and thioformaldehyde by Clouthier and Ramsay,[26] the dipole moments of $CH_2O$ and $CH_2S$ in various electronic states have been determined. The dipole moment of $CH_2S$ is much smaller than that of $CH_2O$, especially in the excited states, where it is on the order of one-third to one-half of the dipole moment of $CH_2O$. The stronger dipole moment indicates that $CH_2O$ accumulates more negative charge on the O atom, thereby increasing the electrostatic interaction between $Fe^+$ and $CH_2O$. On the other hand, for $Fe(CH_2S)^+$, the dative interaction between iron and sulfur, particularly ligand to metal donation, determines the covalent bond nature of $Fe^+-CH_2S$. The back-donation in $Fe^+-SCH_2$ further weakens the C−S bond, as evidenced by the calculated bond length. As a result, $Fe(CH_2S)^+$ undergoes structural reorganization, while $Fe(CH_2O)^+$ does not.

## Summary

The gas-phase reactions of $Fe(CH_2O)^+$ and $Fe(CH_2S)^+$ with small alkanes show significant differences in the reactivities and reaction mechanisms. While C−C insertion leading to alkane loss is predominant for the reactions of $Fe(CH_2O)^+$, C−H insertion is preferred for $Fe(CH_2S)^+$. $CH_2O$ behaves like a spectator ligand and the reactivity of $Fe(CH_2O)^+$ is similar to $Fe^+$. On the other hand, $CH_2S$ ligand participates in rearrangement to form an activated $H_2S-Fe^+-$olefin complex, which then dissociates by elimination of $H_2S$. From CID and ion−molecule reactions, $D^0(Fe^+-CH_2S)$ is found to be in the range of 37 ± 2 to 49.6 ± 2.3 kcal/mol and $D^0(Fe^+-CH_2O)$ is less than 34 ± 2 kcal/mol, the latter being consistent with other determinations. Density functional calculations help elucidate the chemical bonding in the two metal−ligand systems and yield metal ion−ligand binding energies, which are in excellent agreement with experimental values, as well as provide an explanation of the experimental results.

**Acknowledgment** is made to the Division of Chemical Sciences in the Office of Basic Energy Sciences in the United States Department of Energy (under grant DE-FG02−87ER13766) for supporting this research. The authors thank Prof. Peter Armentrout for useful correspondence. The authors also appreciate the reviewers for their constructive suggestions.

JA964234N